

## Heteroligand copper(I) $\pi$ -complex of 1-allyl-1*H*-benzotriazole and pyridine: synthesis, crystal structure and Hirshfeld surface analysis

Yurii SLYVKA<sup>1\*</sup>, Evgeny GORESHNIK<sup>2</sup>, Marian MYS'KIV<sup>1</sup>

<sup>1</sup> Department of Inorganic Chemistry, Ivan Franko National University of Lviv, Kyryla i Mefodiya St. 6, 79005 Lviv, Ukraine

<sup>2</sup> Department of Inorganic Chemistry and Technology, Jožef Stefan Institute, Jamova St. 39, SI-1000 Ljubljana, Slovenia

\* Corresponding author. Tel.: +380-32-2394506; e-mail: yurii.slyvka@lnu.edu.ua

Received December 9, 2016; accepted December 28, 2016; available on-line April 1, 2018

By means of the alternating current electrochemical technique, a new heteroligand  $[\text{Cu}_2\text{Cl}_2(1\text{-Abtr})(\text{Py})]_2$  complex (1-*Abtr* = 1-allyl-1*H*-benzotriazole, *Py* = pyridine) has been obtained and characterized by X-ray single crystal diffraction. Crystals of the title compound are monoclinic, space group  $P2_1/n$ ,  $a = 10.6059(10)$ ,  $b = 8.9848(7)$ ,  $c = 17.1098(17)$  Å,  $\beta = 97.798(5)^\circ$ ,  $V = 1615.3(3)$  Å<sup>3</sup> at 293 K,  $Z = 2$ . Dimeric  $[\text{Cu}_2\text{Cl}_2(1\text{-Abtr})(\text{Py})]_2$  fragments are formed in the structure. The 1-*Abtr* moiety acts as a chelate-bridging ligand, being attached to the copper(I) ions via two triazole N atoms and the olefin C=C bond of the ligand allyl group. The two copper atoms have distinctly different coordination environments:  $\pi$ -bonded Cu(I) ion adopts an approximately trigonal pyramidal surrounding, which includes a pyridine N atom, and the  $\sigma$ -bonded copper(I) ion a distorted tetrahedral surrounding, formed by two triazole N atoms and two bridging halogen ions. To visualize the interactions between the fragments a Hirshfeld surface analysis was performed.

### 1,2,3-Triazole / Pyridine / Copper(I) / $\pi$ -Complex / Crystal structure

#### 1. Introduction

1,2,3-Triazoles form a well-known class of heterocycles, which presents a huge range of biological activity and photophysical properties, and finds applications in materials chemistry as well as in crystal engineering of organometallic compounds [1-3]. The existence of an olefin C=C bond attached to the skeleton of the 1,2,3-triazoles serves as the actual key for the coordination of transition metal ions, due to metal-olefin  $\pi$ -bonding [4,5]. Specific contribution of N-allylbenzotriazole to the unusual Cu(I) coordination abilities was found in the  $[\text{Cu}_2(\text{C}_9\text{H}_9\text{N}_3)_2(\text{H}_2\text{O})_2\text{SiF}_6] \cdot 2\text{H}_2\text{O}$   $\pi$ -complex (in which rare  $\text{Cu}^1 \dots \text{F}(\text{SiF}_6^{2-})$  interaction was observed [6]) and in the  $[\text{Cu}(\text{C}_9\text{H}_9\text{N}_3)(\text{HSO}_4)]$  compound, which may be the first known example of a  $\text{CuHSO}_4$   $\pi$ -complex. The coordination abilities of 1-allylbenzotriazole towards copper(I) halides have been studied in the case of two crystalline  $\pi$ -compounds,  $[\text{Cu}_2(1\text{-Abtr})_2\text{Cl}_2]$  (1-*Abtr* = 1-allyl-1*H*-benzotriazole ( $\text{C}_9\text{H}_9\text{N}_3$ )) and  $[\text{Cu}_2(1\text{-Abtr})_2\text{Cl}_{1.7}\text{Br}_{0.3}]$  (in which 1-*Abtr* molecule acts as N,(C=C)-bidentate bridging ligand), and one  $\sigma$ -complex,  $[\text{Cu}(1\text{-Abtr})\text{Br}]$  [7-9]. In order to examine the Cu(I) complexation with N-allylbenzotriazole in the presence of a N-donor co-ligand such as pyridine,

we undertook the synthesis and structure characterization of the original heteroligand  $\pi$ -complex  $[\text{Cu}_2\text{Cl}_2(1\text{-Abtr})(\text{Py})]_2$  (**1**) (1-*Abtr* = 1-allyl-1*H*-benzotriazole ( $\text{C}_9\text{H}_9\text{N}_3$ ) and *Py* = pyridine ( $\text{C}_5\text{H}_5\text{N}$ )).

#### 2. Experimental section

##### 2.1 Synthesis of N-allylbenzotriazole

N-allylbenzotriazole was prepared from commercially available benzotriazole, freshly distilled allyl chloride, and  $\text{NaHCO}_3$  in ethanol, in accordance with the procedure described in [10]. The <sup>1</sup>H NMR spectrum of the ligand agreed well with earlier reported data and showed the presence of both 1- (1-*Abtr*) and 2-isomers (2-*Abtr*) of N-allylbenzotriazole in an approximately equimolar ratio.

##### 2.2 Preparation of $[\text{Cu}_2\text{Cl}_2(1\text{-Abtr})(\text{Py})]_2$ (**1**)

Crystals of the complex **1** were obtained under the conditions of an alternating-current electrochemical synthesis [11], starting from a pyridine solution of the 1-*Abtr* and 2-*Abtr* mixture and  $\text{CuCl}_2 \cdot 2\text{H}_2\text{O}$ . The solution was placed into a small 5 mL test-tube and then copper-wire electrodes in cork were inserted.

After application of an alternating-current tension (frequency 50 Hz) of 0.54 V for 6 days good-quality colorless crystals of **1** appeared on the copper electrodes.

### 2.3 X-ray crystal structure determination

Diffraction data for a crystal of **1** were collected on a Rigaku AFC7 diffractometer equipped with a Mercury CCD area detector and graphite-monochromatized Mo  $K\alpha$  radiation. The collected data were processed with the Rigaku CrystalClear software suite program package [12]. The structure was solved by direct methods using SHELXS-97, and refined by the least-squares method on  $F^2$  by SHELXL-97 software, implemented in the program package WinGX [13-16]. The non-hydrogen atoms were found by direct methods and the hydrogen atoms geometrically. A full-matrix least-squares refinement based on  $F^2$  was carried out for the positional and displacement parameters of all the non-hydrogen atoms. The positions of the H atoms were treated as riding ones and refined with fixed C–H distances and with  $U_{\text{iso}}(\text{H})$  values set to  $1.2U_{\text{eq}}(\text{C})$ . The figures were prepared using DIAMOND 3.1 software [17]. The crystal parameters, data collection and refinement are summarized in Table 1. Fractional atomic coordinates and displacement atomic parameters for **1** are listed in Table 2.

### 3. Results and discussion

The reaction of CuCl (appearing *in situ* under *ac* electrochemical conditions) with the 1-allyl (1-*Abtr*) and 2-allylbenzotriazole (2-*Abtr*) mixture in pyridine solution leads to isomer-selective complexation of  $\text{Cu}^+$  with 1-*Abtr* exclusively, resulting in the heteroligand  $[\text{Cu}_2\text{Cl}_2(1\text{-Abtr})(\text{Py})]_2$  (**1**)  $\pi$ -complex. The complex **1**

crystallizes in the centrosymmetric space group  $P2_1/n$  and is built up from large centrosymmetric  $\{\text{Cu}_2\text{Cl}_2(1\text{-Abtr})(\text{Py})\}_2$  fragments (Fig. 1 and Fig. 2), connected through weak C–H...Cl hydrogen bonds into a framework. The crystallographically independent part of **1** includes two copper(I) atoms (Cu1 and Cu2), two chlorine atoms (Cl1 and Cl2) one 1-allylbenzotriazole (1-*Abtr*) molecule, and one pyridine (*Py*) molecule. The 1-*Abtr* moiety acts as chelate-bridging ligand, being attached to the copper(I) ions *via* two triazole N atoms and the olefin C=C bond of the ligand allyl group. The two copper atoms have distinctly different coordination environments. Cu1 adopts a distorted tetrahedral ( $\tau_4 = 0.88$ ) surrounding ( $\tau_4$  is the four-coordinate geometry index [18]), including two bridging Cl atoms and two triazole N atoms of two neighboring organic molecules. Cu2 adopts a close to trigonal pyramidal ( $\tau_4 = 0.74$ ) surrounding, including a pyridine N atom, a C=C bond of 1-*Abtr*, and one of the halogen atoms (Cl1) in the basal plane of the polyhedron. The second halogen atom, apically bonded to Cu2, is located at 2.842(2) Å from the metal atom, which is significantly shorter than the sum of the van der Waals radii of Cu and Cl reported by Bondi [19,20] (3.15 Å) and very much shorter than the corresponding sum of 4.20 Å, recently proposed by Alvarez [21]. The Cu1–Cu2 distance (2.973(2) Å) is too long for metallophilic interaction. Cu1 acts as a bridge, connecting two symmetry-related  $\{\text{Cu}_2\text{Cl}_2(1\text{-Abtr})(\text{Py})\}$  fragments into a  $\{\text{Cu}_2\text{Cl}_2(1\text{-Abtr})(\text{Py})\}_2$  dimer by means of Cu–N bonds.

It is interesting to note that **1** is topologically reminiscent of the  $[\text{Cu}(1\text{-Abtr})\text{Br}]$   $\sigma$ -complex, in which centrosymmetric  $\{[\text{Cu}(1\text{-Abtr})]_2\}^{2+}$  dimers (having one six-member  $\{\text{Cu}_2\text{N}_4\}$  ring) are bonded *via* bridging bromide anions into infinite chains [9].

**Table 1** Crystal data and structure refinement for **1**.

Empirical formula	$\text{C}_{28}\text{H}_{28}\text{Cl}_4\text{Cu}_4\text{N}_8$	$F(000)$	872
Formula weight, g/mol	872.58	Color, shape	colorless, block
Temperature, K	293(2)	Theta range for data collection, °	2.6–29.1
Wavelength, Å	0.71069	Limiting indices	$-3 \leq h \leq 13, -10 \leq k \leq 12, -21 \leq l \leq 15$
Crystal system, space group	monoclinic, $P2_1/n$	Refinement method	Full-matrix least-squares on $F^2$
Unit cell dimensions:		Measured reflections	4548
<i>a</i> , Å	10.6059(10)	Unique reflections	3063
<i>b</i> , Å	8.9848(7)	Reflections with $I > 2\sigma(I)$	2234
<i>c</i> , Å	17.1098(17)	Free parameters	199
$\alpha$ , °	90	Goodness-of-fit on $F^2$	1.13
$\beta$ , °	97.798(5)	<i>R</i> values	$R_1 = 0.068, wR_2 = 0.197$
$\gamma$ , °	90	Largest difference peak and hole, $e/\text{Å}^3$	1.12 and –0.79
<i>V</i> , Å <sup>3</sup>	1615.3(3)	Calculated density, g/cm <sup>3</sup>	1.794
<i>Z</i>	2		
Absorption coeff., mm <sup>–1</sup>	2.96		

**Table 2** Fractional atomic coordinates and (equivalent) isotropic displacement parameters ( $\text{\AA}^2$ ) for **1**.

Atom	<i>x</i>	<i>y</i>	<i>z</i>	$U_{\text{iso}}/U_{\text{eq}}^a$
Cu1	0.36914(7)	0.03857(9)	0.92633(5)	0.0402(3)
Cu2	0.08862(8)	-0.00506(9)	0.90115(6)	0.0454(3)
Cl1	0.2001(2)	0.1096(2)	1.0060(1)	0.0424(4)
Cl2	0.2755(2)	0.0408(2)	0.7992(1)	0.0420(4)
N1	0.4902(5)	-0.1826(5)	1.0391(3)	0.035(1)
N2	0.4050(5)	-0.1639(6)	0.9772(4)	0.040(1)
N3	0.3297(5)	-0.2844(5)	0.9675(3)	0.032(1)
N4	-0.0185(5)	0.1646(6)	0.8530(4)	0.044(1)
C1	0.4720(5)	-0.3222(6)	1.0713(4)	0.032(1)
C2	0.5398(6)	-0.3946(7)	1.1357(4)	0.036(1)
H2	0.6102	-0.3519	1.1657	0.044
C3	0.4953(7)	-0.5343(8)	1.1519(4)	0.045(2)
H3	0.5356	-0.5863	1.1952	0.053
C4	0.3914(6)	-0.6001(7)	1.1050(4)	0.037(2)
H4	0.3664	-0.6952	1.1179	0.044
C5	0.3251(6)	-0.5301(7)	1.0407(4)	0.038(2)
H5	0.2562	-0.5745	1.01	0.045
C6	0.3684(6)	-0.3871(6)	1.0245(4)	0.033(1)
C7	0.2303(6)	-0.2965(7)	0.9005(4)	0.037(1)
H71	0.219	-0.4006	0.8864	0.045
H72	0.258	-0.2452	0.8559	0.045
C8	0.1035(6)	-0.2333(6)	0.9149(4)	0.036(1)
H81	0.0872	-0.2192	0.9665	0.043
C9	0.0120(6)	-0.1963(7)	0.8537(4)	0.042(2)
H91	0.0273	-0.2100	0.8019	0.051
H92	-0.0655	-0.1576	0.8639	0.051
C11	-0.1464(7)	0.1609(8)	0.8496(4)	0.045(2)
H11	-0.1841	0.0792	0.8704	0.054
C12	-0.2229(7)	0.2749(9)	0.8159(4)	0.050(2)
H12	-0.3109	0.2689	0.8132	0.060
C13	-0.1670(8)	0.3981(9)	0.7864(5)	0.060(2)
H13	-0.2170	0.4761	0.7639	0.072
C14	-0.0376(8)	0.4038(8)	0.7905(5)	0.060(2)
H14	0.002	0.4853	0.7708	0.072
C15	0.0332(7)	0.2857(8)	0.8245(5)	0.050(2)
H15	0.1213	0.2905	0.8279	0.060

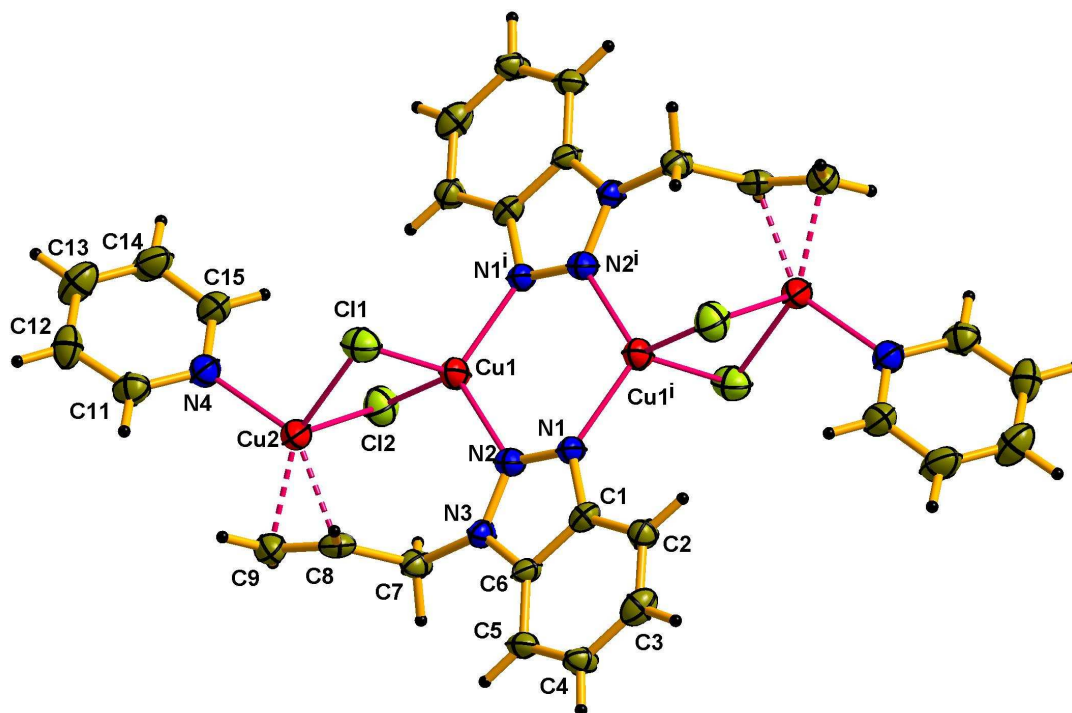
<sup>a</sup> For non-hydrogen atoms  $U_{\text{eq}}$  is defined as one-third of the trace of the orthogonalized  $U_{ij}$  tensor, for hydrogen atoms  $U_{\text{iso}} = 1.2U_{\text{eq}}(\text{C})$ .

For comparison, in the earlier studied  $[\text{Cu}_2(1\text{-Abtr})_2\text{Cl}_2]$  and  $[\text{Cu}_2(1\text{-Abtr})_2\text{Cl}_{1.7}\text{Br}_{0.3}]$  [7,8] compounds, the 1-*Abtr* molecules connect  $\text{Cu}^+$  ions through  $\mu_2\text{-C}_3\text{N}_3$ -bridges into infinite  $\{[\text{Cu}(1\text{-Abtr})]^+\}_n$  chains, and the latter are coupled *via* bridging  $\text{Cl}^-$  anions in geminate chains. The additional coordination of the pyridyl N atom to  $\text{Cu}^+$  in **1** prevents the formation of chains, resulting in finite  $\{\text{Cu}_2\text{Cl}_2(1\text{-Abtr})(\text{Py})\}_2$  dimeric fragments with two seven-membered  $\{\text{Cu}_2\text{N}_2\text{C}_2\text{Cl}\}$  rings and one six-membered  $\{\text{Cu}_2\text{N}_4\}$  ring.

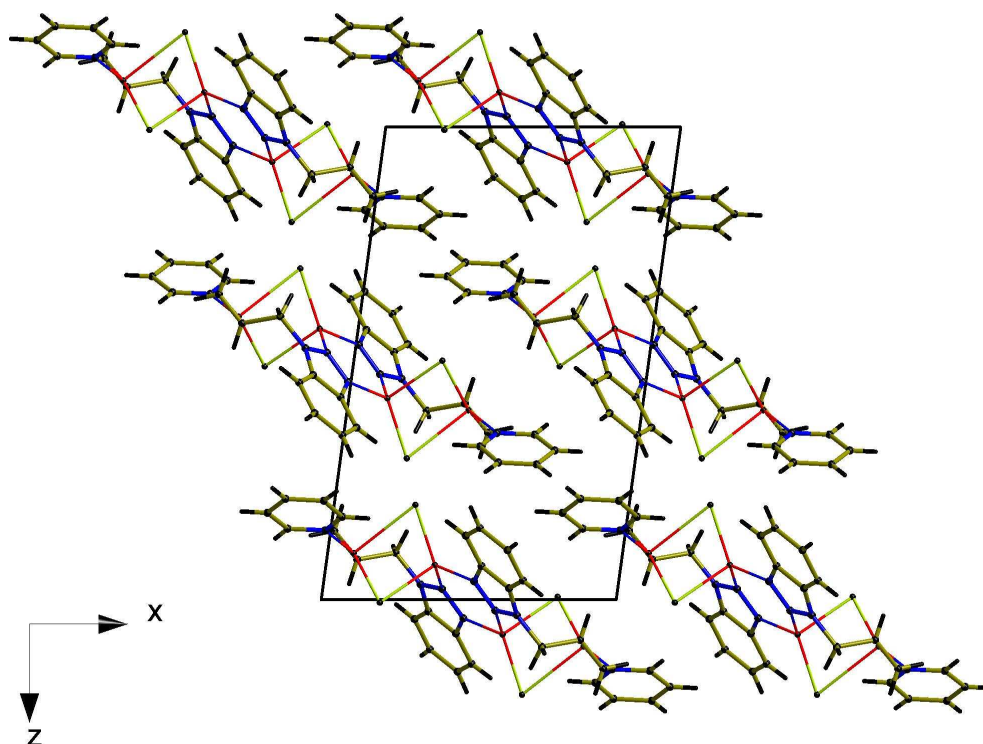
The double C8=C9 bond in **1** is slightly elongated to 1.369(9)  $\text{\AA}$  (due to the effective  $\pi$ -dative  $\text{Cu}(\text{I}) \rightarrow (\text{C}=\text{C})_\pi$  component of the  $\pi$ -bond), in comparison to an unbound double bond of 1.33  $\text{\AA}$ . The efficiency of the  $\text{Cu}(\text{I})-(\text{C}=\text{C})$  interaction is confirmed by the fact that the angle between the C=C

bond and the base plane of the Cu2 trigonal pyramid is 1.0°. The rather short Cu–*m* (*m* is the middle point of the C=C bond) distance and rather large C–Cu–C angle (Table 3) also confirm this conclusion. The 1-allylbenzotriazole ligand in **1** is also involved in  $\pi\cdots\pi$  and H...C interactions, arising from weak bonding between 1-*Abtr* molecules, as well as between 1-*Abtr* and *Py* molecules of neighboring  $[\text{Cu}_2\text{Cl}_2(1\text{-Abtr})(\text{Py})]_2$  fragments.

Isomer-selective complexation of Cu(I) towards N-allylbenzotriazole in the presence of ionic copper(I) salts (such as  $\text{CuClO}_4$ ,  $\text{CuBF}_4$  or  $\text{CuHSO}_4$ ), has been studied previously [10]. The reaction of these copper salts with an 1-*Abtr* and 2-*Abtr* mixture under *ac*-conditions results in the formation of complexes with 2-allylbenzotriazole, which fully uses its coordination abilities, playing a chelate-bridging role.



**Fig. 1** Centrosymmetric  $[\text{Cu}_2\text{Cl}_2(1\text{-Abtr})(\text{Py})]_2$  fragment in **1**. Symmetry code: (i)  $1-x, -y, 2-z$ .

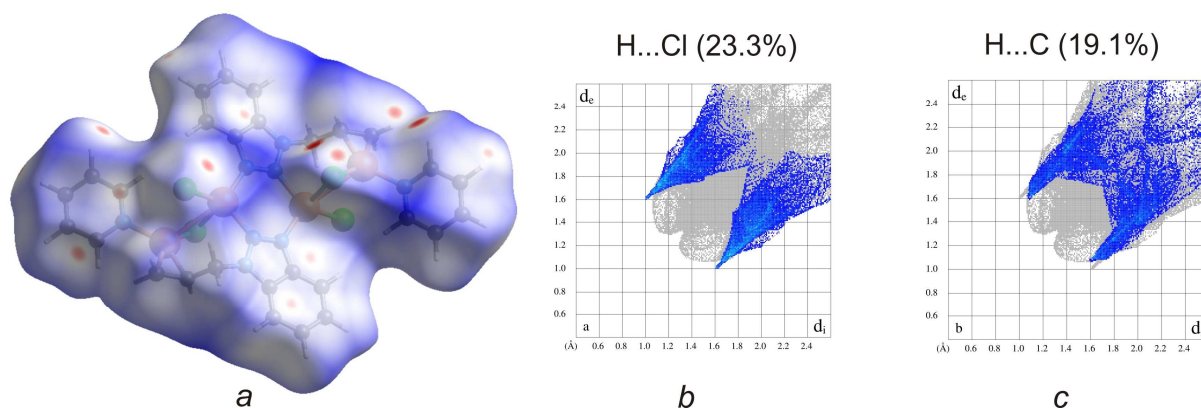


**Fig. 2** Crystal packing of **1** along the  $[010]$  direction.

**Table 3** Selected bond lengths (in Å) and angles (in deg) in the structure of **1**.

Bond	Value	Angle	Value
Cu1–Cl1	2.478(2)	N2–Cu1–Cl1	95.9(2)
Cu1–Cl2	2.265(2)	N2–Cu1–Cl2	116.9(2)
Cu1–N2	2.031(6)	N2–Cu1–N1 <sup>i</sup>	111.3(2)
Cu1–N1 <sup>i a</sup>	2.003(5)	C11–Cu1–N1 <sup>i</sup>	103.7(2)
Cu2–Cl1	2.258(2)	C11–Cu1–Cl2	105.65(7)
Cu2–Cl2	2.842(2)	N4–Cu2–Cl1	100.7(2)
Cu2–N4	2.010(6)	N4–Cu2–Cl2	92.3(2)
Cu2– <i>m</i> <sup>b</sup>	1.928(6)	N4–Cu2– <i>m</i>	127.2(3)
C8–C9	1.369(9)	C11–Cu2– <i>m</i>	128.7(2)
N1–N2	1.307(7)	C11–Cu2–Cl2	95.03(7)
N2–N3	1.341(7)	C7–C8–C9	121.4(6)
N4–C15	1.339(9)	C8–Cu2–C9	39.1(3)

<sup>a</sup> Symmetry code: (i) 1–*x*, –*y*, 2–*z*;

<sup>b</sup> *m* – midpoint of the C8=C9 bond.


**Fig. 3** Hirshfeld surface analysis of the  $[\text{Cu}_2\text{Cl}_2(1\text{-Abtr})(\text{Py})]_2$  dimer in **1**. (a) Hirshfeld surface mapped with  $d_{\text{norm}}$  which highlights both donor and acceptor ability. (b) Fingerprint plot of crystal fragment resolved into H...Cl contacts. (c) Fingerprint plot of crystal fragment resolved into H...C contacts. The full fingerprint appears beneath each decomposed plot in grey.

It is well known that the chelate effect strongly increases the stability of a complex, for this reason, in the presence of weakly bonded  $\text{ClO}_4^-$ ,  $\text{BF}_4^-$  and  $\text{HSO}_4^-$  anions (because of the high accessibility of the metal center), 2-*Abtr* coordination is more favorable than 1-*Abtr*. Instead, 1-*Abtr* is a more suitable ligand for the only bridging coordination mode because of the higher spatial accessibility of the N1 atom of the triazole core. This is the main reason why only the 1-*Abtr* derivative selectively reacts with the copper(I) halides.

#### 4. Hirshfeld surface analysis

The Hirshfeld surface was built for the  $[\text{Cu}_2\text{Cl}_2(1\text{-Abtr})(\text{Py})]_2$  fragment in **1** to analyze the interactions between the moieties. The most prominent interactions between H atoms and Cl atoms, as well as the C...H and C...C interactions between neighboring fragments, can be seen in the

Hirshfeld surface plot as bright- and pale-red areas (Fig. 3). Fingerprint plots were produced to show the intermolecular surface bond distances with the regions of H...Cl and H...C interactions highlighted. The contribution to the surface area for C...C contacts is 5.0 % and for H...H contacts 39.1 %.

#### References

- [1] J. Totobenazara, A.J. Burke, *Tetrahedron Lett.* 56 (2015) 2853-2859.
- [2] F.H. Allen, *Acta Crystallogr. B* 58 (2002) 380-388.
- [3] T. Gazivoda Kraljević, A. Harej, M. Sedić, S. Kraljević Pavelić, V. Štepanić, D. Drenjančević, J. Talapko, S. Raić-Malić, *Eur. J. Med. Chem.* 124 (2016) 794-808.
- [4] E. Goreshnik, G. Veryasov, D. Morozov, Yu. Slyvka, B. Ardan, M. Myskiv, *J. Organomet. Chem.* 810 (2016) 1-11.

- [5] Y. Slyvka, E. Goreshnik, O. Pavlyuk, M. Mys'kiv, *Cent. Eur. J. Chem.* 11 (2013) 1875-1901.
- [6] E.A. Goreshnik, Yu.I. Slyvka, M.G. Mys'kiv, *Inorg. Chim. Acta* 377 (2011) 177-180.
- [7] E.A. Goreshnik, *Pol. J. Chem.* 73 (1999) 1253-1258.
- [8] E.A. Goreshnik, B.M. Mykhalichko, V.N. Davydov, *J. Struct. Chem.* 46 (2005) 172-176.
- [9] Yu. Slyvka, E. Goreshnik, M. Mys'kiv, *Chem. Met. Alloys* 9 (2016) 61-65.
- [10] E.A. Goreshnik, A.A. Vakulka, Yu.I. Slyvka, M.G. Mys'kiv, *J. Organomet. Chem.* 710 (2012) 1-5.
- [11] B.M. Mykhalichko, M.G. Mys'kiv, Ukraine Patent UA 25450A, Bull. 6, 1998.
- [12] *CrystalClear*, Rigaku Corporation, The Woodlands, Texas, USA, 1999.
- [13] A. Altomare, G. Cascarano, C. Giacovazzo, A. Guagliardi, M.C. Burla, G. Polidori, M. Camalli, *J. Appl. Crystallogr.* 27 (1994) 435-436.
- [14] *TeXan for Windows*, version 1.06, Crystal Structure Analysis, Package, Molecular Structure Corporation, 1997-1999.
- [15] G.M. Sheldrick, *Acta Crystallogr. A* 64 (2008) 112-122.
- [16] L.J. Farrugia, *J. Appl. Crystallogr.* 32 (1999) 837-838.
- [17] *DIAMOND v3.1*, Crystal Impact GbR, Bonn, Germany, 2004-2005.
- [18] L. Yang, D.R. Powell, R.P. Houser, *Dalton Trans.* (2007) 955-964.
- [19] A. Bondi, *J. Phys. Chem.* 68 (1964) 441-451.
- [20] A. Bondi, *J. Phys. Chem.* 70 (1966) 3006-3007.
- [21] S. Alvarez, *Dalton Trans.* 42 (2013) 8617-8636.